Journal of Magnetic Resonance **142,** 276–279 (2000)
doi:10.1006/jmre.1999.1954, available online at http://www.idealibrary.com on IDEAL®

New ^{15}N NMR Exchange Experiments for the Unambiguous Assignment of $^{1}H^{N}/^{15}N$ Resonances of Proteins in Complexes in Slow Chemical Exchange with Free Form

Catherine Vialle-Printems, Carine van Heijenoort, and Eric Guittet[1]

Laboratoire de RMN, ICSN–CNRS, 1 Avenue de la Terrasse, F-91198 Gif-sur-Yvette, France

Received May 5, 1999; revised September 27, 1999

The potentialities of a 2D proton-detected heteronuclear exchange experiment to assign the nitrogen and amide proton resonances in a uniformly ^{15}N-enriched macromolecule involved in a complex, starting from the free form assignments, are demonstrated on a protein–DNA complex. This 2D experiment is further extended to a 3D experiment in the case of severe superpositions. © 2000 Academic Press

Key Words: **chemical exchange; heteronuclear 3D NMR; AlcR; protein; complex.**

Structural studies of DNA–protein or protein–protein complexes by NMR are rather arduous and can hardly be carried out without uniformly isotope-enriched biomolecule samples. Moreover, such studies usually start with the elucidation of the structure of at least one component of the complex, in its free form. For systems in slow intermolecular exchange on the NMR chemical shift time scale, resonances of the already assigned free form of the macromolecule and the bound form of the corresponding part of the complex can be correlated through proton chemical exchange spectroscopy (*1*). Because of the extensive dipolar cross polarization effects present in proton experiments, either intramolecular or intermolecular, 2D proton-detected heteronuclear experiments are preferable. Various experimental schemes have been proposed to monitor slow intramolecular conformational exchanges (*2–4*) but, so far, they have not been applied for systems in slow intermolecular exchange. We propose here the extension of one such 2D experiment to a 3D experiment to unambiguously assign the nitrogen and amide proton resonances in a uniformly ^{15}N-enriched macromolecule involved in a complex, starting from the free protein assignments.

During the mixing time of exchange experiments, chemical exchange, longitudinal relaxation, and cross relaxation occur. Our interest here is not the exchange relaxation rate measurement but the unambiguous assignment of the resonances of the bound state. We therefore want to minimize the contribution of the last two phenomena. The ^{15}N–^{15}N dipolar cross relaxation is proportional to $(\gamma_{15_N})^4$ leading to a peak $(\gamma_{1_H}/\gamma_{15_N})^4$, i.e., 10^4 times weaker than the one due to ^{1}H–^{1}H nuclear Overhauser effects (NOE). Contrary to what happens in the ^{1}H–^{1}H exchange experiment, the corresponding cross peaks are thus negligible. Heteronuclear experiments are thus more appropriate to monitor a slow conformational exchange. They can be divided into two classes where the slow conformational exchange can be monitored either by the chemical exchange of heteronuclear longitudinal two-spin-order states, I_zS_z, (*2, 3*) or by the net transfer of heteronuclear S_z (*2, 4*). The ^{15}N (S_z) longitudinal auto relaxation rate is usually much slower than the one of a two-spin-order state I_zS_z. A ^{15}N (S_z) exchange experiment thus allows the analysis of exchanges over a wider rate range than a (I_zS_z) exchange experiment, where the detected signal is weakened by longitudinal relaxation during the mixing time. This phenomenon is even stronger for a ^{1}H (I_z) exchange experiment. A ^{15}N (S_z) exchange experiment is thus best suited for the present application.

The pulse sequence of the 2D ^{15}N-exchange experiment is similar to those designed for T_1 heteronuclear relaxation rate measurements (*5–7*) and is also similar to experiments designed to monitor slow conformational exchanges (*2–4*). The pulse sequence is shown in Fig. 1. This ^{1}H–^{15}N reverse ^{15}N–^{15}N exchange experiment provides an additional, nondiagonal, ^{15}N dimension with proton sensitivity. Moreover, a complete analysis of the sequence using the product operator formalism shows that no contribution due to the heteronuclear (^{15}N–^{1}H) NOE is detected.

The intensities of the auto peaks and exchange peaks of an exchange spectrum have already been described (*1*). The maximal intensity for the exchange cross peaks is obtained for $\tau_{opt} = 1/2D \ln[(\sigma + D)/(\sigma - D)]$ with $D = \sqrt{\delta^2 + x_b x_f k_{ex}^2}$, $\sigma = 0.5(k_{ex} + R_{1f} + R_{1b})$, $\delta = 0.5[(x_f - x_b)k_{ex} + R_{1b} - R_{1f}]$. The chemical exchange rate is k_{ex}. R_{1f} is the ^{15}N longitudinal relaxation rate of the free protein and R_{1b} is the ^{15}N longitudinal relaxation rate of the bound protein. We have to point out that R_{1b} is not necessarily known at this stage of the study of the complex. Therefore τ_{opt} must be chosen in such a range that, on the first hand, R_{1b}

[1] To whom correspondence should be addressed. Fax: (33) 169823784. E-mail: guittet@icsn.cnrs-gif.fr.

1090-7807/00 $35.00

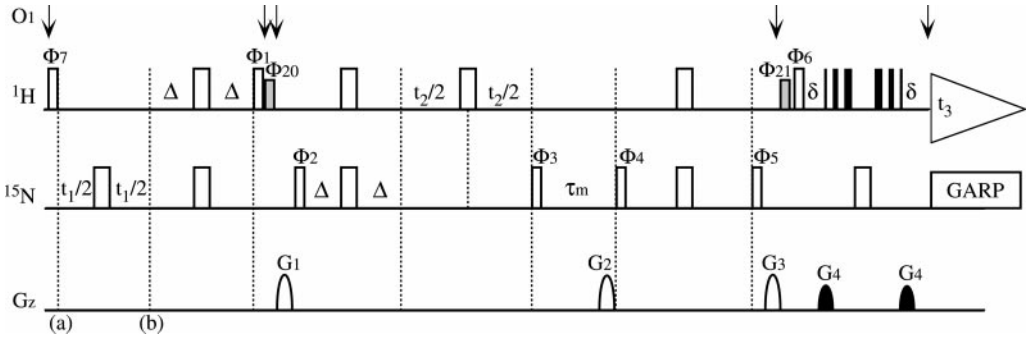

FIG. 1. Pulse sequence of the 3D ^{15}N exchange experiment. The 2D experiment pulse sequence is obtained by omitting the subsequence (a–b) and replacing phase Φ_7 by x. Narrow and wide bars represent 90° and 180° pulses, respectively. Gray bars represent 90° water selective flip-back ^{1}H pulses which ensure better water suppression (*11*). Unless otherwise specified, all pulses are applied along the $+x$ axis. Phase cycle elements are $\Phi_1 = 2(y), 2(-y)$; $\Phi_2 = x, -x$; $\Phi_3 = 2(y, -y, -y, y), 2(-y, y, y, -y)$; $\Phi_4 = 4(x, -x), 4(-x, x)$; $\Phi_5 = 2(y), 2(-y)$; $\Phi_6 = 4(x), 4(-x)$; $\Phi_7 = x$; $\Phi_{20} = x$; $\Phi_{21} = 4(x), 4(-x)$; and $\Phi_r = x, 2(-x), x, -x, 2(x), -x$. The delay Δ is set to $1/4J = 2.75$ ms. A mixing time τ_m of 150 ms is applied. All gradient pulses are sine-bell-shaped with a duration of 800 μs and are applied along the z axis with $G_1 = 8$ G/cm, $G_2 = 22$ G/cm, $G_3 = 31$ G/cm, and $G_4 = 17$ G/cm. Each gradient is followed by a 45-μs recovery time. ^{15}N decoupling during acquisition is achieved via a GARP sequence (*12*) with a RF field strength of 2.27 kHz. Quadrature detection in t_1 (2D) or t_2 (3D) is achieved according to States–TPPI (*13*) by incrementing the phase Φ_2. The ^{1}H carrier is alternatively set at the water frequency and at the center of the amide proton region. The carrier shifts are represented by arrows. Water signal suppression is achieved by an on-resonance WATERGATE sequence (*14, 15*). δ is set according to Ref. (*15*). A relaxation delay of 2 s is used between each transient. The first two ^{15}N 180° pulses in the proton frequency evolution period t_1 can be concatenated (*16*).

has a value compatible with the size and the would-be dynamics of the complex, and on the second hand, that the auto peaks and the exchange peaks remain of comparable and observable intensities. The range of likely applicability of this experiment in terms of binding affinity can be readily estimated. The lifetime of the complex must be of the same order as the mixing time (a few tens of milliseconds), thus leading to an estimation of the off-rate around 10–100 s^{-1} and, assuming a diffusion-controlled reaction, of the equilibrium dissociation constant in the micromolar range.

The pulse sequence has been used on the ^{15}N-labeled DNA-binding domain of the alcohol regulator protein AlcR, complexed with a DNA target. AlcR is a transcription factor from *Aspergillus nidulans* required for the activation of the genes encoding the ethanol metabolizing enzymes. The AlcR fragment studied here consists of 65 amino acids with a zinc cluster motif of the Cys-X2-Cys-X6-Cys-X16-Cys-X2-Cys-X6-Cys type (*8*) and its NMR spectra have been assigned in our laboratory. We also have established that the AlcR DNA-binding domain binds to a 10-mer DNA duplex bearing the 5′-TACGG-3′ consensus sequence with a 1:1 stoichiometry. The measured lifetime of the AlcR complex is 74 ± 7 ms, with a dissociation constant in the micromolar range (*9*). The protein:DNA stoichiometry used for our 2D exchange experiment is a 2:1 stoichiometry, leading to a 1:1 ratio for the bound and free states of the protein. An optimal mixing time of 150 ms was evaluated based on the measured mean R_{1f} value of 1.6 s^{-1} and an estimated R_{1b} value of 1 s^{-1}. Comparison of the free protein HSQC, the bound protein HSQC, and the 2D exchange experiment leads to a partial assignment of the bound protein HSQC (Fig. 2). It should be noted that only NH groups are detected; NH_2 groups can be specifically detected, using a scheme similar to the one used for the specific measurement of T_1 relaxation of NH_2 groups (*10*). Some amino acids, such as C22, D23, Rϵ28, and C39, present unambiguous exchange correlations between the auto peaks. For these peaks, both H^N and ^{15}N frequencies are different, creating well-defined square patterns. In other cases only lines, either rows or columns, are seen. This means that only one of the two resonances (H^N or ^{15}N) is shifted between the free and the DNA-bound protein. Auto and exchange peaks are superimposed. Such row patterns are clearly observed for G18, G35, and S40, for which ^{15}N chemical shifts do not vary upon binding. The corresponding peaks could be unambiguously assigned here because there is no ambiguity due to any superposition. A symmetric case appears when the ^{15}N resonance alone varies, as is the case for C12. A few other peaks like C49 and T50 are superimposed on the free and DNA-bound protein spectra. A straightforward assignment in such cases is only possible in the absence of overlaps, but due to the complexity of the spectra, most resonances remain unassigned. A 3D experiment is then useful to go further in the assignment procedure.

The 3D experiment proposed here takes up again the 2D exchange pulse scheme but the proton to nitrogen transfer is now preceded by an evolution of the proton magnetization. The 3D spectrum obtained is a ($^1H^N$, ^{15}N, $^1H^N$) cube (see Fig. 3). The desired magnetization transfer is now described by the scheme

$$H_{Ni} \rightarrow H_{Ni}(t_1) \rightarrow N_i(t_2) \xrightarrow{\tau_m} \begin{cases} N_j \rightarrow H_{Nj}(t_3) \\ N_i \rightarrow H_{Ni}(t_3). \end{cases}$$

This scheme was chosen because the 2D exchange spectrum

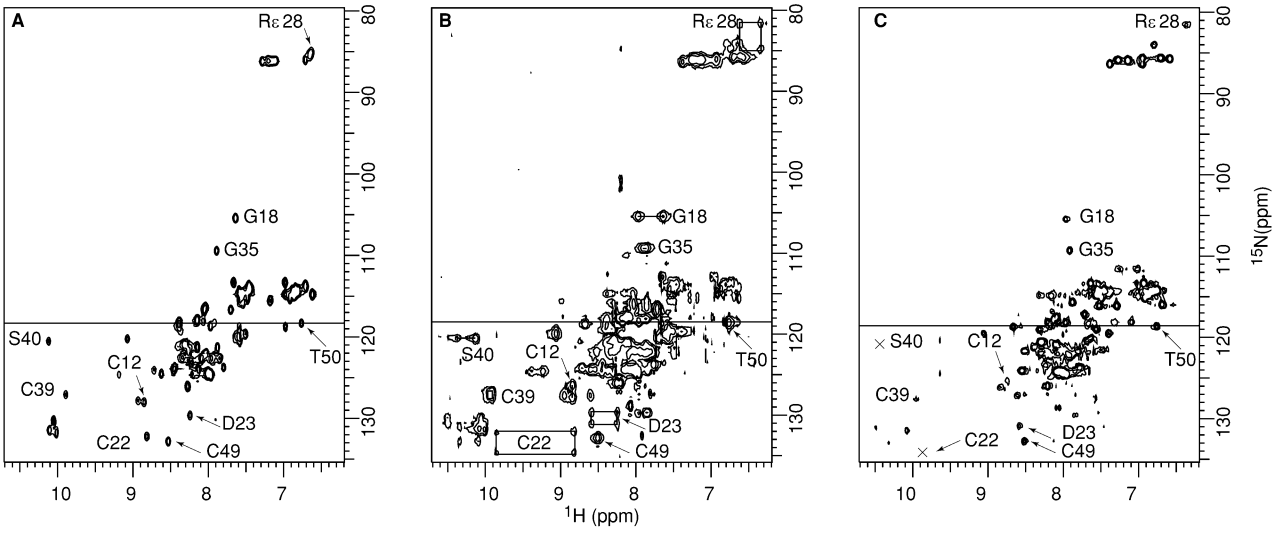

FIG. 2. (A) HSQC spectrum of free AlcR. (B) 2D ^{15}N exchange spectrum of AlcR–DNA (protein:DNA 2:1). (C) HSQC spectrum of bound AlcR (protein:DNA 1:2). Spectral widths were 5000 Hz in both dimensions for the 2D exchange experiment. The total experimental time was 86 h with 128 complex t_1 points, 512 complex t_2 points, 512 scans per FID, and a relaxation delay of 2 s. Data were multiplied by a pure cosine window function in t_1 and a pure squared-cosine window function in t_2 prior to Fourier transformation. Final data matrix size was 256(R)*1024(R), R meaning real points. AlcR solution concentrations were about 2 mM for the free AlcR sample and exactly 1.6 mM for both protein:DNA samples. Exact protein and DNA concentrations were measured by fluorescence (*17*). The same buffer was used for all samples (10 mM sodium phosphate, 0.1 M NaCl, pH 6.0) in H_2O/D_2O 95:5 (v/v). All spectra were acquired at 20°C on a Bruker AMX spectrometer using a triple-resonance $^1H^{13}C^{15}N$ probehead with a self-shielded *z*-gradient coil. Data were processed with GIFA software (*18*). ^{1}H chemical shifts are referenced to trimethylsilylpropionate. ^{15}N chemical shifts are referenced to external $^{15}NH_4Cl$ (2.9 M in 1 M Hcl at 20°C) at 24.93 ppm. Some of the connectivities observed are shown in solid lines. The peak broadness of the exchange spectrum (B) is due to the exchange of transverse magnetization during t_1 and t_2. The poor signal-to-noise ratio of the bound AlcR spectrum (C) is due to partial degradation. Peaks of weak intensities are shown by an X.

suggests that binding affects H^N chemical shifts more than ^{15}N chemical shifts. Thus, the H^N chemical shift evolution time was chosen to resolve exchange peaks with ^{15}N superimposed resonances. Four cases can be distinguished. In case (i), only the ^{15}N chemical shift is different between the two states of the protein (Fig. 3, upper left). In case (ii), both H^N and ^{15}N chemical shifts are equal in both states of the protein (Fig. 3, upper right). The 3D experiment provides no further information compared to the 2D experiment in these two cases. In case (iii), both the free protein H^N and the ^{15}N chemical shifts vary between the free and the bound protein. This case creates a square pattern in the 2D experiment. The 3D experiment spreads the information and can therefore facilitate the assignment in crowded regions (Fig. 3, lower left). In case (iv), only the H^N chemical shift varies. In the 2D experiment, the fact that the free and bound auto peaks have the same ^{15}N chemical shifts leads to a superposition of auto and exchange peaks, whereas in the 3D experiment exchange peaks are brought to light (Fig. 3, lower right). Auto and exchange peaks lie in the same plane perpendicular to the F_2 (^{15}N) dimension leading to a square pattern. This ^{15}N plane has one of its two dimensions (the acquisition dimension) well resolved. This is the choice case for the proposed 3D experiment, allowing definite assignments, which are impossible with the 2D experiment. The example of Lys 47 is given in Fig. 4.

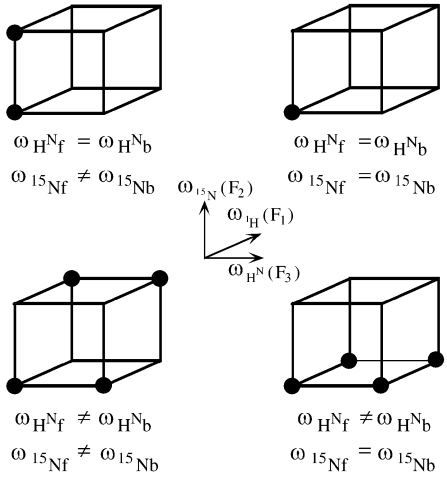

FIG. 3. Theoretical 3D ^{15}N exchange spectrum for the different cases discussed in the text. Black dots represent resonance peaks. f and b subscripts stand for free and bound.

An alternative scheme can also be proposed, where the second evolution period is introduced after the mixing period, leading to a (^{15}N, ^{15}N, $^1H^N$) spectrum. The best application of such an experiment would be in the case of H^N superimposed resonances, which seems less frequent here. Moreover, square patterns would be observed on a plane perpendicular to F_3 with

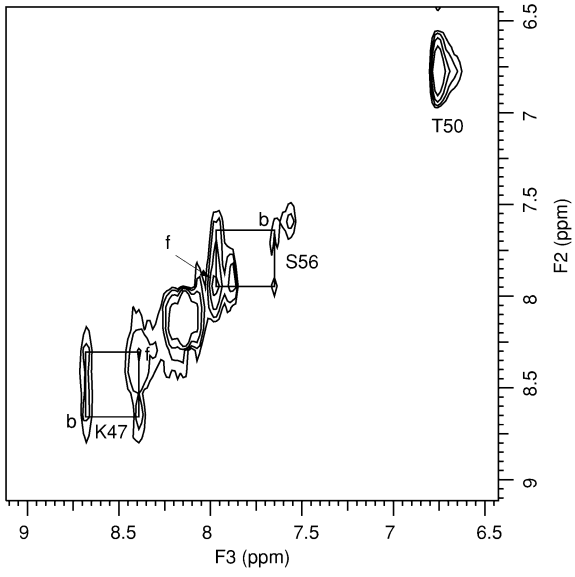

FIG. 4. Slice of 3D ^{15}N-exchange spectrum, corresponding to the ^{15}N resonance shown by dashed lines in Fig. 2. The 3D spectrum was acquired with the pulse sequence shown in Fig. 1. Spectral widths were 5000 Hz in the ω_2 dimension (^{15}N) and 9259.26 Hz in the ω_1 and ω_3 dimensions (^{1}H). 32(C)*32(C)*512(C) points were acquired with 32 scans per FID, leading to a total experimental time of 86 h; C means complex points. Data were multiplied with a pure cosine window function in ω_1 and ω_2 dimensions and a pure squared-cosine window function in the acquisition dimension. Forward linear prediction to 64 complex data points in both t_1 and t_2 dimensions was used prior to apodization and Fourier transformation. Final data matrix size was 128(R)*128(R)*1024(R). This slice shows the square pattern correlating free (f) and DNA-bound (b) K47 (see text, case ii). The second square is presumed to be S56. The 3D experiment allows us to distinguish both amino acids and correlate their free and bound peaks.

two poorly resolved dimensions. This could hamper the unambiguous assignment of correlated resonances.

The method proposed here will greatly facilitate the assignment of the $H^N/^{15}N$ resonances of a biomolecule in a complex, knowing its free form assignment. We illustrated this method with a complex composed of a DNA-binding domain and its DNA target. About 65% of the residues could be assigned unambiguously following our strategy, mainly from the analysis of the 3D experiment, affording a valuable basis to perform the complete assignment of the protein in the complex using more standard 3D heteronuclear experiments. Strong assumptions could be made for the left 35% of the residues, which were confirmed by the analysis of 2D nuclear Overhauser effect spectra (NOESY). The analysis of the chemical shift variations upon binding gives valuable indications on the residues located at the interface of the two partners in the complex.

REFERENCES

1. J. Jeener, B. H. Meier, P. Bachmann, and R. R. Ernst, Investigation of exchange processes by two-dimensional NMR spectroscopy, *J. Chem. Phys.* **71,** 4546–4553 (1979).
2. G. T. Montelione and G. Wagner, 2D chemical exchange NMR spectroscopy by proton-detected heteronuclear correlation, *J. Am. Chem. Soc.* **111,** 3096–3098 (1989).
3. G. Wider, D. Neri, and K. Wüthrich, Studies of slow conformational equilibria in macromolecules by exchange of heteronuclear longitudinal 2-spin-order in a 2D difference correlation experiment, *J. Biomol. NMR* **1,** 93–98 (1991).
4. N. A. Farrow, O. Zhang, and J. D. Forman-Kay, and L. E. Kay, A heteronuclear correlation experiment for simultaneous determination of ^{15}N longitudinal decay and chemical exchange rates of systems in slow equilibrium, *J. Biomol. NMR* **4,** 727–734 (1994).
5. D. P. Burum and R. R. Ernst, Net polarisation transfer via a *J*-ordered state for signal enhancement of low sensibility nuclei, *J. Magn. Reson.* **39,** 163–168 (1980).
6. N. R. Nirmala and G. Wagner, Measurement of ^{13}C relaxation times in proteins by two-dimensional heteronuclear ^{1}H–^{13}C correlation spectroscopy, *J. Am. Chem. Soc.* **110,** 7557–7558 (1988).
7. L. E. Kay, D. A. Torchia, and A. Bax, Backbone dynamics of proteins as studied by ^{15}N inverse detected heteronuclear NMR spectroscopy: Application to staphylococcal nuclease, *Biochemistry* **28,** 8972–8979 (1989).
8. P. Kulmburg, N. Judewicz, M. Mathieu, F. Lenouvel, D. Sequeval, and B. Felenbok, Specific DNA binding sites for the activator protein, ALCR, in the *alcA* promotor of the ethanol regulon of *Aspergillus nidulans, J. Biol. Chem.* **267,** 1–8 (1992).
9. R. Cerdan, D. Collin, F. Lenouvel, B. Felenbok, and E. Guittet, The *Aspergillus nidulans* transcription factor AlcR forms a stable complex with its half-site DNA: A NMR study, *FEBS Lett.* **408,** 235–240 (1997).
10. J. Boyd, Measurement of ^{15}N relaxation data from the side chains of asparagine and glutamine residues in proteins, *J. Magn. Reson. B* **107,** 279–285 (1995).
11. (a) S. Grzesiek and A. Bax, The importance of not saturing H_2O in protein NMR. Application to sensitivity enhancement and NOE measurements, *J. Am. Chem. Soc.* **115,** 12593–12594 (1993). (b) S. Grzesiek and A. Bax, Measurement of amide proton exchange rates and NOEs with water in ^{13}C/^{15}N-enriched calcineurin B, *J. Biomol. NMR* **3,** 627–638 (1993).
12. A. J. Shaka, P. B. Baker, and R. Freeman, Conmputer-optimized decoupling scheme for wideband applications and low-level operation, *J. Magn. Reson.* **64,** 547–552 (1985).
13. D. Marion, M. Ikura, R. Tschudin, and A. Bax, Rapid recording of 2D NMR spectra without phase cycling. Application to the study of hydrogen exchange in proteins, *J. Magn. Reson.* **85,** 393–399 (1989).
14. M. Piotto, V. Saudek, and V. Sklenár, Gradient tailored excitation for single-quantum NMR spectroscopy of aqueous solutions, *J. Biomol. NMR* **2,** 661–665 (1992).
15. V. Sklenár, M. Piotto, R. Leppik, and V. Saudek, Gradient-tailored water suppression for ^{1}H–^{15}N HSQC experiments optimized to retain full sensitivity, *J. Magn. Reson. A* **102,** 241–245 (1993).
16. G. T. Montelione, B. A. Lyons, S. D. Emerson, and M. Tashiro, An efficient triple resonance experiment using carbon-13 isotropic mixing for determining sequence-specific resonance assignments of isotopically-enriched proteins, *J. Am. Chem. Soc.* **114,** 10974–10975 (1992).
17. P. Pajot, Fluorescence of proteins in 6-M guanidine hydrochloride, *Eur. J. Biochem.* **63,** 263–269 (1976).
18. J.-L. Pons, T. E. Malliavin, and M.-A. Delsuc, Gifa v.4: A complete package for NMR data processing, *J. Biomol. NMR* **8,** 445–452 (1996).